ELSEVIER

Journal of Molecular Structure (Theochem) 625 (2003) 265–275

THEO CHEM

www.elsevier.com/locate/theochem

Ab initio conformational study of caffeic acid

E. VanBesien[a], M.P.M. Marques[b,c,*]

[a]*Dep. Chemie, Katholieke Univ. Leuven, 3001 Heverlee, Belgium*
[b]*Unidade I&D "Química-Física Molecular", Universidade de Coimbra, 3000 Coimbra, Portugal*
[c]*Dep. Bioquímica, Faculdade de Ciências e Tecnologia, Universidade de Coimbra, 3000 Coimbra, Portugal*

Received 21 November 2002; revised 23 December 2002; accepted 6 January 2003

Abstract

A complete conformational analysis of caffeic acid, a phenolic derivative with well known antioxidant properties, was carried out by ab initio calculations, at the density funtional theory (DFT) level. Fourteen different conformers were obtained, the most stable ones being planar, as the conformational preferences of this molecule were found to be mainly determined by the stabilising effect of π-electron delocalisation. Harmonic vibrational frequencies, as well as potential energy profiles for rotation around several bonds within the molecule, were also calculated.

Keywords: Caffeic acid; Ab initio calculations; Conformational analysis

1. Introduction

Phenolic acid derivatives constitute a group of natural compounds present in human diet in significant amounts, which have long been known to display both antioxidant (through their radical scavenging activity) and pro-oxidant properties. They are involved in many metabolic reactions and are naturally occurring in many plant-derived food products, were they are largely responsible for the browning process [1–3]. This kind of compounds is becoming of increasing importance in applied science. In fact, apart from being widely used as antioxidant food additives [4,5], they have also attracted much attention in medical research, as some of them were lately found to display anti-inflammatory and anti-mutagenic effects, or even anti-tumoral activity in different human cancer cell lines [6–11]. In addition, several phenolic esters are candidates to be used as drugs in the prevention of cardiovascular diseases [12,13]. Actually, while dietary antioxidants, such as vitamins E and C, have long received considerable attention in this regard, relatively little is known about a similar antioxidant activity of plant-derived polyphenolic compounds, such as the flavonoids and the phenolic acids.

The knowledge of the conformational preferences of this type of compounds is thus of the utmost importance as a starting point for future studies aiming at the understanding of the structure-activity relationships underlying their

* Corresponding author. Tel.: +351-239-853-600; fax: +351-239-853-607.
E-mail address: pmc@ci.uc.pt (M.P.M. Marques).

0166-1280/03/$ - see front matter © 2003 Elsevier Science B.V. All rights reserved.
doi:10.1016/S0166-1280(03)00026-5

biological activity. Nevertheless, the reported ab initio molecular orbital calculations on phenolic acid derivatives are very scarce, semiempirical quantum-chemical methods being commonly used instead. In fact, apart from these only a few ab initio studies on phenolic antioxidants is to be found in the literature [14–18], one of them on several *p*-hydroxycinnamic acid derivatives, including caffeic acid [18]. However, these studies aim exclusively at the explanation of the structural dependency of the antioxidant activity of this kind of phenolic analogues, focusing only on their most stable geometries.

The goal of the present study, in turn, is to perform a thorough conformational analysis of caffeic acid (3,4-dihydroxy-*trans*-cinnamic acid, CA). Density functional methods—B3LYP/6-31G**—were used, in order to carry out a full geometry optimisation, along with rotational energy profile and harmonic vibrational frequency calculations, yielding all the minimum energy conformations of this molecule.

2. Computational methods

The ab initio calculations—full geometry optimisation and calculation of the harmonic vibrational frequencies—were performed using the GAUSSIAN 98W program [19], within the Density Functional Theory (DFT) approach, in order to properly account for the electron correlation effects (particularly important in this kind of systems). The widely employed hybrid method denoted by B3LYP [20–25], which includes a mixture of HF and DFT exchange terms and the gradient-corrected correlation functional of Lee, Yang and Parr [26,27], as proposed and parametrized by Becke [28,29], was used, along with the double-zeta split valence basis sets 6-31G* and 6-31G** [30,31].

Molecular geometries were fully optimised by the Berny algorithm, using redundant internal coordinates [32]: The bond lengths to within ca. 0.1 pm and the bond angles to within ca. 0.1. The final root-mean-square (rms) gradients were always

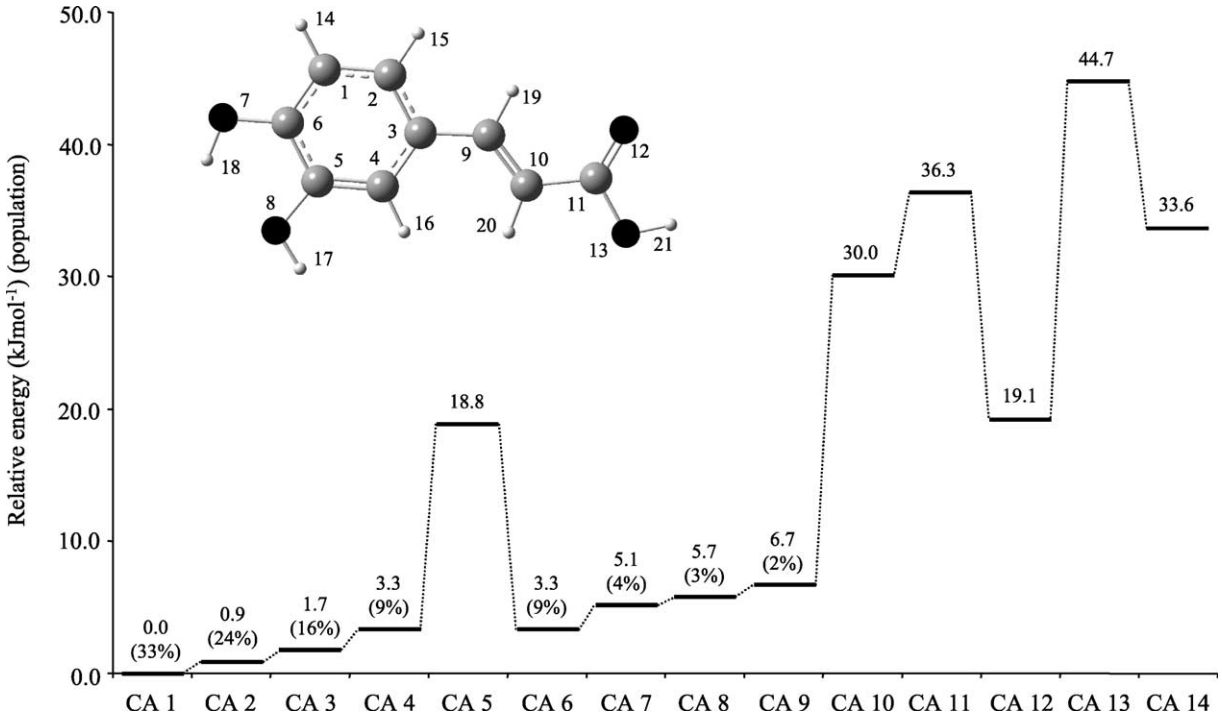

Fig. 1. Schematic representation of the calculated (B3LYP/6-31G**) conformational energies (and populations, at 25 °C) for caffeic acid. (The atom numbering is included).

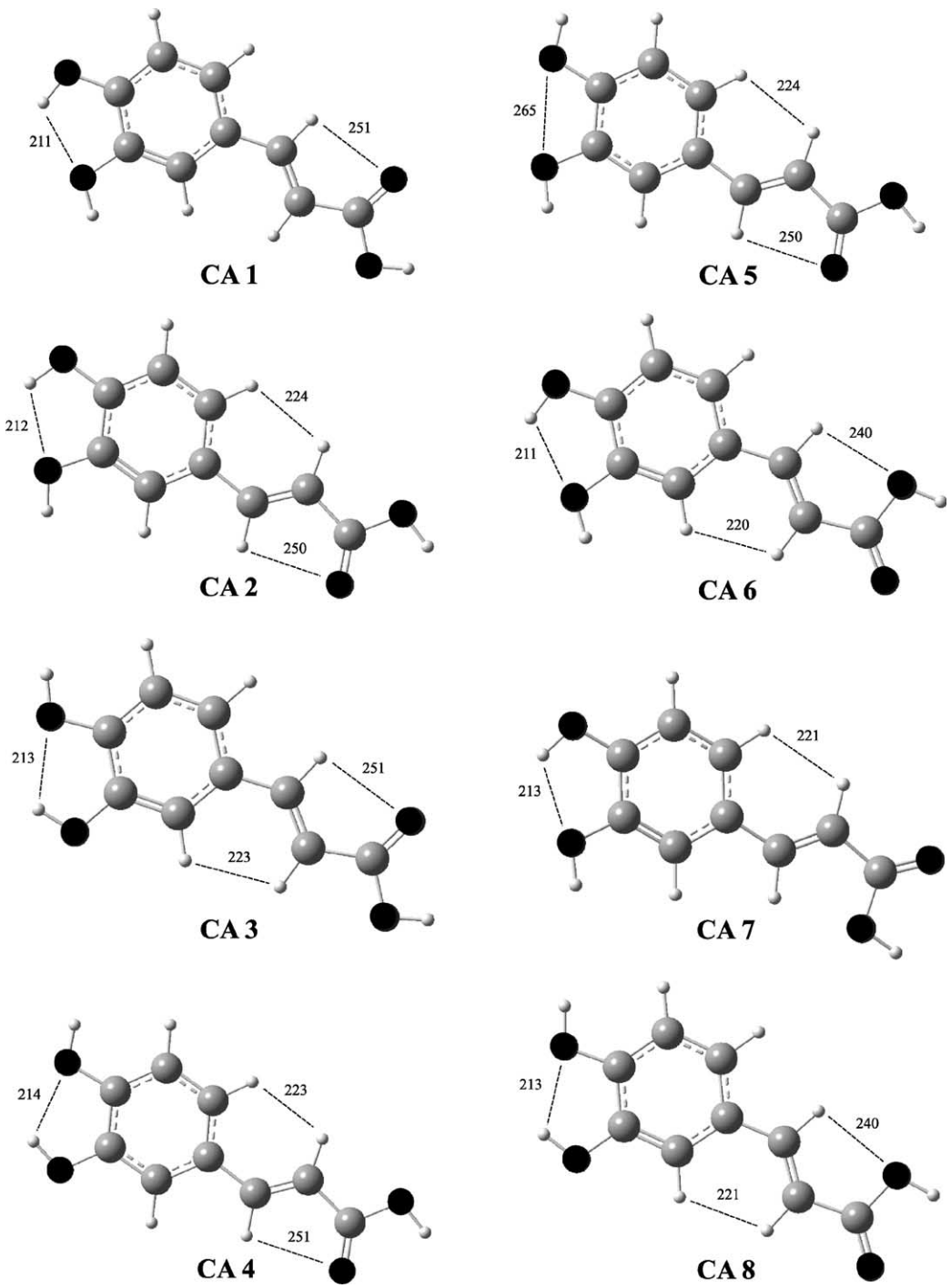

Fig. 2. Schematic representation of the conformers calculated for caffeic acid–displaying (C)H···:O and (O)H···:O intramolecular interactions. (B3LYP/6-31G** level of calculation. Intramolecular distances are represented in pm).

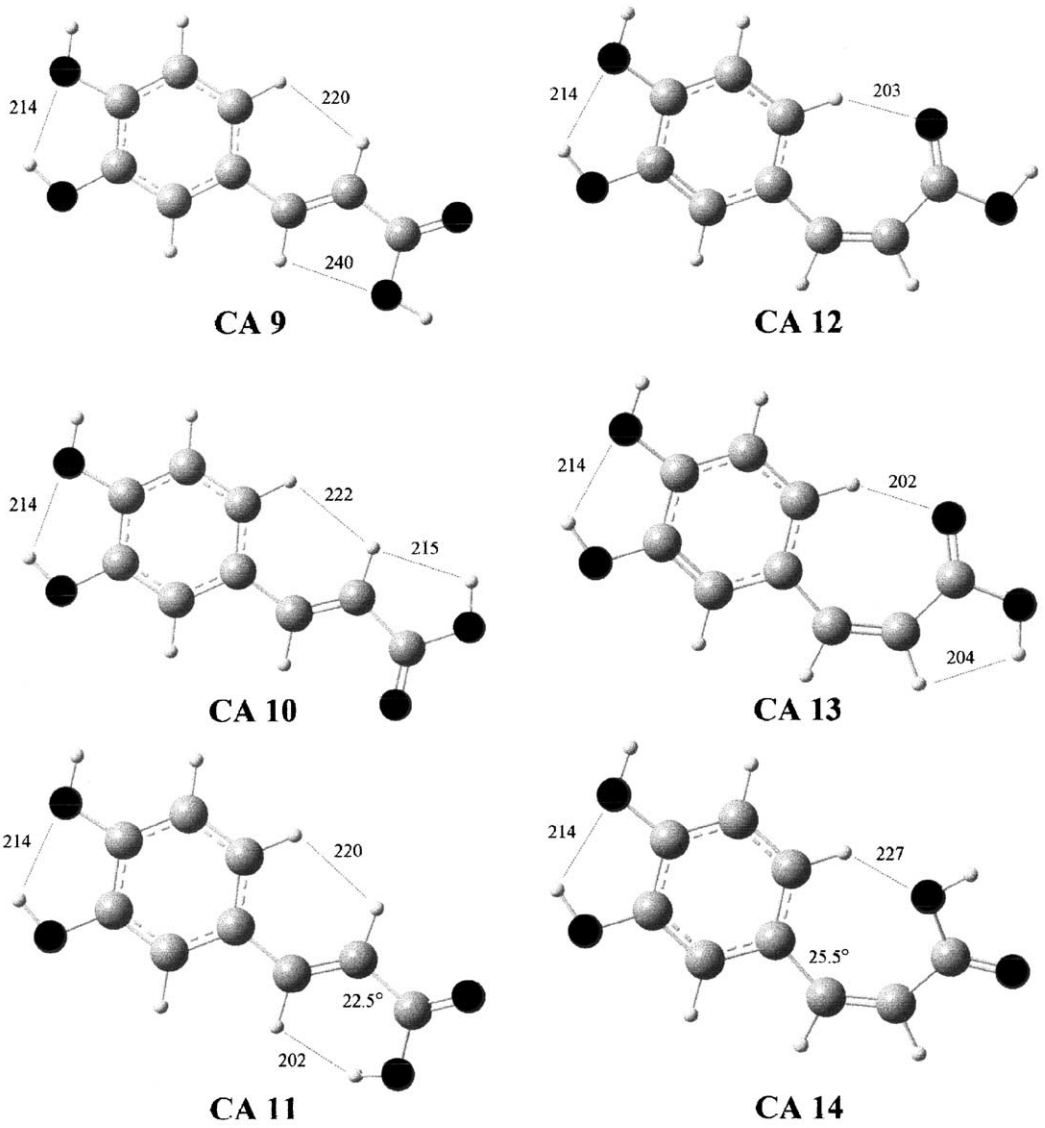

Fig. 2 (*continued*)

less than 3×10^{-4} hartree bohr^{-1} or hartree radian^{-1}. No geometrical constraints were imposed on the molecules under study. The 6-31G** basis set was used for all geometry optimisations, while for most of the rotational energy barrier calculations the smaller basis set 6-31G* was found to yield good results. All frequency calculations were run at the B3LYP/6-31G** level and wavenumbers above 400 cm^{-1} were scaled [33] before comparing them with reported experimental data.

Quantitative potential-energy profiles for rotation around different bonds within the molecule were obtained, by scanning the corresponding dihedrals and using least-squares fitted Fourier-type functions of a dihedral angle, τ [34,35]:

$$P = \sum_{n=1}^{3} \frac{1}{2} P_n[1 - \cos(n\tau)] + \sum_{m=1}^{2} \frac{1}{2} P'_m \sin(m\tau) \qquad (1)$$

The parameters P_n and P'_m correspond to potential-energy (V_n and V_m terms), bond-distance or bond-angle

differences relative to a reference value. According to the symmetry of the caffeic acid molecule, the cosine term in 60° was not included in the fitting of the experimental data. The sine terms, which are of significance only for asymmetric functions around 180°, were not considered either.

3. Results and discussion

A complete geometry optimisation was carried out for caffeic acid, in order to obtain the geometries and relative energies of the distinct possible conformers of the molecule. The effect of several geometrical parameters on the overall stability of the molecule was investigated, namely: (i) S-*cis* or S-*trans* conformation of the carboxylic group dihedral ($H_{21}O_{13}C_{11}O_{12}$) (atoms numbered according to Fig. 1) equal to 0° or 180°, respectively; (ii) orientation of the two phenolic hydroxyls (relative to the ring)-dihedrals ($H_{18}O_7C_6C_1$) and ($H_{17}O_8C_5C_4$) equal to 0° or 180°; (iii) relative orientation of the aromatic ring and the carboxylic moiety of the molecule—dihedral ($O_{12}C_{11}C_{10}C_9$) equal to 0° or 180°, and ($C_{11}C_{10}C_9C_3$) equal to 180° or 0°, the former defining a *trans* or *cis* orientation, respectively, of the ring relative to the carboxylate (around the linear chain C=C bond). Rotational isomerism was also investigated for this molecule, by scanning particular dihedral angles, in view of finding the corresponding rotational energy barriers.

Fourteen different conformers were found (Figs. 1 and 2), the most stable ones displaying an S-*cis* conformation of the carboxylic group, along with a *trans* orientation of the phenyl ring relative to the terminal carboxylate. Except for CA 11 ($\Delta E = 36.3$ kJ mol^{-1}, H_{21} being out-of-the-plane) and CA 14 ($\Delta E = 33.6$ kJ mol^{-1}, displaying an out-of-the-plane carboxylate) (Fig. 2) all energy minima have a planar geometry, probably due to the stabilising effect of π-electron delocalisation between the benzene ring and the linear chain C_9–C_{10} and C_{11}–O_{12} double bonds, which is favoured when they all lie in the same plane. Thus, although a C_1 point group symmetry was initially assumed in the calculations, this changed into a C_s one whenever a planar geometry was found to be an energy minimum.

The conformational energy of caffeic acid was found to be highly dependent on the geometry of the carboxylic group—either S-*cis* or S-*trans*—the former being greatly favoured—geometries CA 4 ($\Delta E = 3.3$ kJ mol^{-1}) vs CA 10 ($\Delta E = 30.0$ kJ mol^{-1}), CA 9 ($\Delta E = 6.7$ kJ mol^{-1}) vs CA 11 ($\Delta E = 36.3$ kJ mol^{-1}), or CA 12 ($\Delta E = 19.1$ kJ mol^{-1}) −1) vs CA 13 ($\Delta E = 44.7$ kJ mol^{-1}) (Figs. 1 and 2). Moreover, it was verified that the orientation of the ring hydroxyl groups has an influence on the conformation of the carbon pendant chain: a slightly lower energy is found for geometries where both phenolic hydroxyl groups point to the carbon chain, in the same direction (in-plane with the aromatic ring)—CA 1 ($\Delta E = 0$) vs CA 3 ($\Delta E = 1.7$ kJ mol^{-1}) and CA 2 ($\Delta E = 0.9$ kJ mol^{-1}) vs CA 4 ($\Delta E = 3.3$ kJ mol^{-1}) (Figs. 1 and 2). In fact, whenever these groups display the same orientation an energetically favoured geometry results, probably due to the formation of medium strength intramolecular H-bonds between O_8 and H_{18}, or O_7 and H_{17} (O···H distances between 211 and 214 pm, Fig. 2). As expected, no stable geometry was obtained when both hydroxyl groups are directed towards each other. However, a conformer was found for opposite orientations of these phenolic OH's-CA 5 ($\Delta E = 18.8$ kJ mol^{-1}, $O_7 \cdots O_8$ distance equal to 265 pm, Fig. 2). As to the relative orientation of the terminal carboxylic group relative to the phenolic hydroxyl groups, an *anti* conformation (i.e. the C=O and the ring OH's pointing to opposite sides of the carbon chain) is preferred over a *syn* one, either for a ($C_{10}C_9C_3C_2$) dihedral equal to 0° − CA 4 ($\Delta E = 3.3$ kJ mol^{-1}) vs CA 9 ($\Delta E = 6.7$ kJ mol^{-1}) or for ($C_{10}C_9C_3C_2$) = 180° CA 1 ($\Delta E = 0$) vs CA 6 ($\Delta E = 3.3$ kJ mol^{-1}) (Fig. 2). Consideration of a *cis* orientation of the aromatic ring relative to the carboxylate group (dihedral ($C_{11}C_{10}C_9C_3$) = 0°) led to rather high energy conformers CA 12 ($\Delta E = 19.1$ kJ mol^{-1}), CA 13 ($\Delta E = 44.7$ kJ mol^{-1}) and CA 14 ($\Delta E = 33.6$ kJ mol^{-1}) (Fig. 2) from which CA 12 is stabilised through the occurrence of a (C_{11})$O_{12} \cdots H_{15}$ intramolecular interaction, yielding a 7-membered intramolecular ring. Although a similar hydrogen bond is also formed in conformer 13 ($O_{12} \cdots H_{15}$ distances of 203 and 202 pm in CA 12 and CA 13, respectively), S-*trans* orientation within the carboxylate group in this case leads to a serious

steric hindrance between hydrogens H_{20} and H_{21} ($H_{20}\cdots H_{21}$ equal to 204 pm, Fig. 2).

Table 1 comprises the optimised geometries for the lowest energy conformers found for CA. These structural parameters do not deviate much from the X-ray values found in the literature for caffeic acid [36] (although comparison between results in the solid and in the gas phase must be done with care). Moreover, the values presently obtained for the most stable conformer, CA 1, are in very good accordance with the ones reported by Bakalbassis et al., for the only ground-state geometry calculated by these authors for caffeic acid, at both the HF/6-31 + G* and B3LYP/6-31 + G* levels [18].

Potential-energy profiles for internal rotation around different bonds within the caffeic acid molecule $-O_7-C_6$ and O_8-C_5, C_3-C_9, $C_{10}-C_{11}$, and $C_{11}-O_{13}$ – were obtained, along with the respective rotational energy barriers, by scanning the corresponding torsional angles.

The ($H_{18}O_7C_6C_1$) and ($H_{17}O_8C_5C_4$) dihedrals describe the orientation of the phenolic hydroxyl groups relative to the aromatic ring, i.e. the internal rotation around the O_7-C_6 and O_8-C_5 bonds. From the corresponding potential-energy profiles (Fig. 3 (a) and (b)), it is concluded that a planar geometry of the OH groups relative to the ring is favoured, as long as ($H_{17}O_8C_5C_4$) is equal to 0° $V_1^{180^\circ} = -15.1/29.5$ kJ mol^{-1} vs $V_2^{90^\circ} = 22.3/-3.4$ kJ mol^{-1}, respectively for ($H_{18}O_7C_6C_1$) and ($H_{17}O_8C_5C_4$) angles. However, for different values of ($H_{17}O_8C_5C_4$), the repulsion between atoms H_{17} and H_{18} leads to a preference for a non-planar orientation of the O_8H_{17} group. Scanning of each of these dihedrals was started for a particular conformation of the neighbouring OH group: when scanning ($H_{17}O_8C_5C_4$) the value of ($H_{18}O_7C_6C_1$) was fixed at 180°, while ($H_{17}O_8C_5C_4$) was kept at 0° when scanning ($H_{18}O_7C_6C_1$). Values of 180° and 0° for ($H_{18}O_7C_6C_1$) and ($H_{17}O_8C_5C_4$), respectively, yield a planar, energetically favoured conformation (as previously discussed, e.g. conformers CA1 and CA2), where an intramolecular $(O_7)H_{18}\cdots O_8$ hydrogen bond may be formed ($H_{18}\cdots O_8$ equal to 211 and 212 pm in CA 1 and CA 2, respectively, Fig. 2). Also, the planar geometry displaying both ($H_{18}O_7C_6C_1$) and ($H_{17}O_8C_5C_4$) equal to 0° (CA 5, Fig. 2) is not

Table 1
Energies and optimised geometries for the most stable conformers of caffeic acid (B3LYP/6-31G** level of calculation. The atoms are numbered according to Fig. 1)

ΔE(kJ mol^{-1})/μ(D)[a]	CA 1 0/3.5[b]	CA 2 0.9/2.2	CA 3 1.7/4.3
Bond lengths/pm			
$O_{13}-C_{11}$	136.2	136.1	136.1
$O_{12}=C_{11}$	121.8	121.8	121.8
$O_{13}-H_{21}$	97.2	97.2	97.2
$C_{11}-C_{10}$	147.0	147.1	147.2
$C_{10}=C_9$	134.8	134.8	134.7
C_9-C_3	145.6	145.7	145.9
$C_{10}-H_{20}$	108.5	108.4	108.5
C_9-H_{19}	108.9	108.9	108.9
O_7-C_6	135.6	135.7	137.2
O_8-C_5	137.5	137.6	136.1
O_7-H_{18}	97.0	97.0	96.6
O_8-H_{17}	96.5	96.5	96.9
C_1-C_2	139.3	139.0	139.5
C_2-C_3	140.5	140.7	140.5
C_3-C_4	141.3	141.0	141.0
C_4-C_5	138.3	138.6	138.6
C_5-C_6	141.2	140.7	141.1
C_6-C_1	139.2	139.6	139.0
C_4-H_{16}	108.7	108.8	108.4
C_2-H_{15}	108.6	108.5	108.5
C_1-H_{14}	108.5	108.5	108.7
$O_{13}-C_{11}$	136.2	136.1	136.1
Bond angles/degrees			
$H_{21}-O_{13}-C_{11}$	105.5	105.6	105.6
$O_{13}-C_{11}=O_{12}$	121.9	122.0	122.0
$O_{13}-C_{11}-C_{10}$	111.5	111.5	111.5
$C_{11}-C_{10}=C_9$	120.0	119.8	119.9
$C_{10}=C_9-C_3$	128.2	128.1	128.0
$C_9-C_3-C_2$	118.9	123.5	118.5
$H_{19}-C_9=C_{10}$	116.0	115.8	116.0
$H_{20}-C_{10}=C_9$	123.3	123.3	123.2
$O_8-C_5-C_6$	114.4	114.7	120.2
Dihedral angles/degrees			
$H_{21}-O_{13}-C_{11}-C_{10}$	180.0	180.0	180.0
$O_{12}=C_{11}-C_{10}=C_9$	0.0	0.0	0.0
$O_{13}-C_{11}-C_{10}=C_9$	180.0	180.0	180.0
$C_{11}-C_{10}=C_9-C_3$	180.0	180.0	180.0
$C_{10}=C_9-C_3-C_2$	180.0	180.0	180.0
$C_9-C_3-C_4-C_5$	180.0	180.0	180.0
$H_{20}-C_{10}=C_9-C_3$	0.0	0.0	0.0

[a] $1D = 1/3 \times 10^{-2}$ cm.

[b] Total value of energy (in Hartree, 1 Hartree = 2625.5001 kJ mol^{-1}) for the most stable conformer of caffeic acid is −648.683926651.

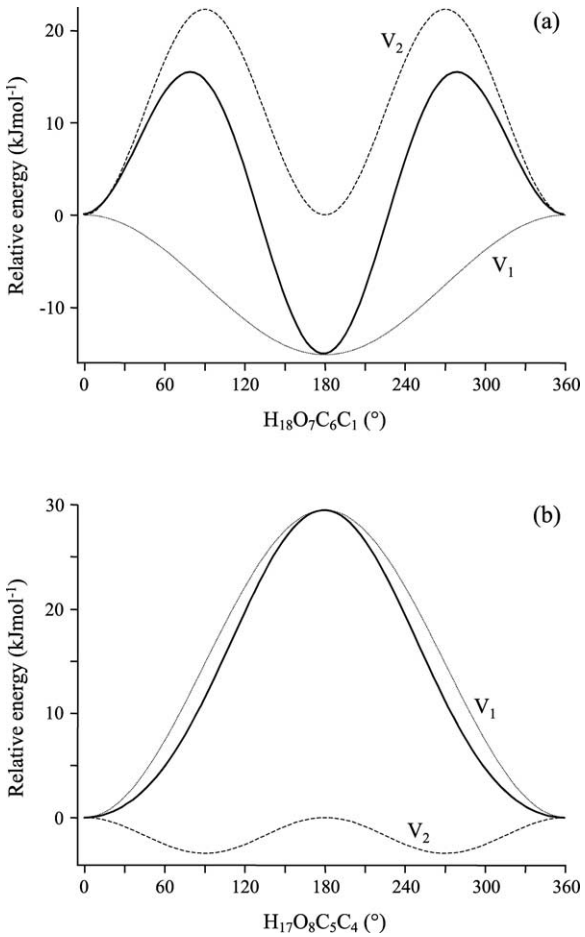

Fig. 3. Optimised conformational energy profiles, and their Fourier deconvolution, for the internal rotation around the O_7-C_6 (a) and O_8-C_5 (b) bonds of caffeic acid. (a)$-V_1 = -15.1$ kJ mol^{-1}, $V_2 = 22.3$ kJ mol^{-1}; (b)-$V_1 = 29.5$ kJ mol^{-1}, $V_2 = -3.4$ kJ mol^{-1}. (($H_{18}O_7C_6C_1$) and ($H_{17}O_8C_5C_4$) were kept at 180° and 0°, respectively, while scanning dihedrals ($H_{17}O_8C_5C_4$) and ($H_{18}O_7C_6C_1$). B3LYP/6-31G** level of calculation).

energetically favoured, owing to some degree of repulsion between atoms O_7 and O_8. Moreover, no stable conformation was found for both ($H_{18}O_7C_6C_1$) and ($H_{17}O_8C_5C_4$) equal to 180°, due to the strong steric hindrance between hydrogens H_{17} and H_{18}. By performing scanning calculations for these same internal rotations without any frozen parameters, a certain amount of cooperativity between the internal rotation of the two phenolic hydroxyls was detected, through small deviations (up to 9°) in the initial values of either dihedral upon variation of the other.

Dihedral ($C_{10}C_9C_3C_2$) defines the position of the pendant carbon chain relative to the benzene ring. The analysis of the Fourier components of the corresponding potential-energy variation (Fig. 4) manifests the preference for a planar geometry of the molecule, i.e. for a completely conjugated system—in fact, the cosine term in 90° (V_2) is by far the primary positive contribution ($V_2^{90^\circ} = 27.6$ kJ mol^{-1} vs $V_1^{180^\circ} = -2.4$ kJ mol^{-1}). A rotational energy barrier of 29.9 kJ mol^{-1}—from ($C_{10}C_9C_3C_2$) equal to 180° to 90° — was obtained. In order to corroborate this strong stabilisation due to π-electron delocalisation, a similar calculation was carried out for the analogous compound to caffeic acid displaying a saturated linear chain (3,4-dihydroxyhydrocinnamic acid, HCA), which yielded a symmetrical potential-energy plot, mainly determined by steric factors: a minimum for ($C_{10}C_9C_3C_2$) = 90°, along with two maxima for both 0° and 180° ($V_1^{180^\circ} = 2.2$ kJ mol^{-1} vs $V_2^{90^\circ} = -7.0$ kJ mol^{-1}).

The variation of the ($O_{12}C_{11}C_{10}C_9$) dihedral (Fig. 5) corresponds to the internal rotation of the carboxylate group relative to the rest of the molecule, around the $C_{10}-C_{11}$ bond. The term in 90° was found to be the ruling contribution ($V_2^{90^\circ} = 42.0$ kJ mol^{-1} vs $V_1^{180^\circ} = -1.8$ kJ mol^{-1}), the planar arrangement of the carboxylate group relative to the aromatic ring and

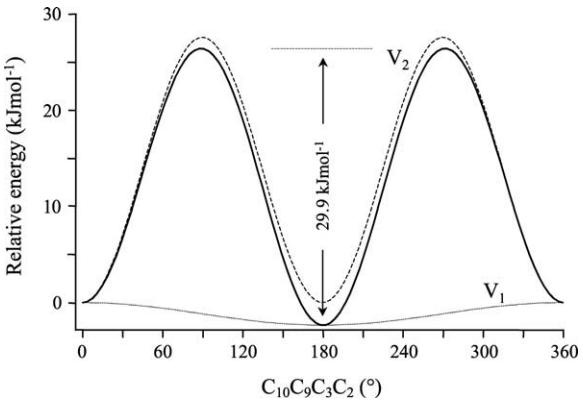

Fig. 4. Optimised conformational energy profile, and its Fourier deconvolution, for the internal rotation around the C_9-C_3 bond of caffeic acid. $V_1 = -2.4$ kJ mol^{-1}, $V_2 = 27.6$ kJ mol^{-1}. (B3LYP/6-31G** level of calculation).

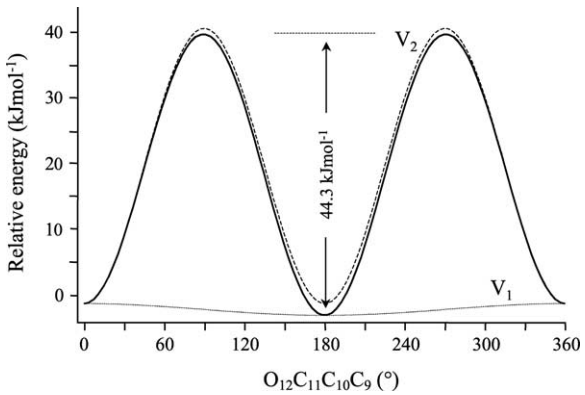

Fig. 5. Optimised conformational energy profile, and its Fourier deconvolution, for the internal rotation around the $C_{11}-C_{10}$ bond of caffeic acid. $V_1 = -1.8$ kJ mol^{-1}, $V_2 = 42.0$ kJ mol^{-1}. (B3LYP/6-31G** level of calculation).

the carbon chain double bond being once more highly favoured ($\Delta E = 44.3$ kJ mol^{-1}). Rotation around the $C_{11}-O_{13}$ bond (variation of the $(H_{21}O_{13}C_{11}C_{10})$ dihedral angle), defining either an S-*cis* or S-*trans* conformation within the carboxylic group, is represented in Fig. 6, and corresponds to the highest energy barrier calculated for this molecule ($\Delta E = 56.0$ kJ mol^{-1}). The clear preference for an S-*cis* orientation is reflected in the potential-energy values obtained, the less favoured conformation being

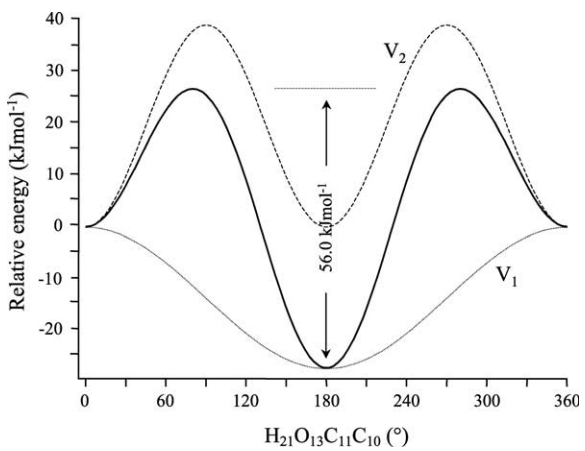

Fig. 6. Optimised conformational energy profile, and its Fourier deconvolution, for the internal rotation around the $O_{13}-C_{11}$ bond of caffeic acid. $V_1 = -27.4$ kJ mol^{-1}, $V_2 = 39.3$ kJ mol^{-1}. (B3LYP/6-31G** level of calculation).

the one with $(H_{21}O_{13}C_{11}C_{10}) = 90°$, due to the loss of planarity of the system $-V_2^{90°} = 39.3$ kJ mol^{-1} vs $V_1^{180°} = -27.4$ kJ mol^{-1}. In fact, it is interesting to note that the S-*trans* geometry is not the energy maximum, as it corresponds to a planar arrangement of the molecule, in spite of the possibility of existence of a certain amount of steric hindrance between hydrogen atoms H_{20} and H_{21} (e.g. $H_{20}\cdots H_{21}$ ca. 215 pm in CA 10, Fig. 2). It is thus concluded that the most stable conformation of the carboxylate group in caffeic acid is the one displaying values of 0° and 180° for the $(O_{12}C_{11}C_{10}C_9)$ and $(H_{21}O_{13}C_{11}C_{10})$ dihedrals, respectively (e.g. lowest energy geometries CA1, CA2 and CA3, as discussed above).

Fig. 7 represents the dependence of the $(C_2C_3C_9)$ and $(C_3C_9C_{10})$ bond-angles on the rotation around the C_9-C_3 bond within the caffeic acid molecule.

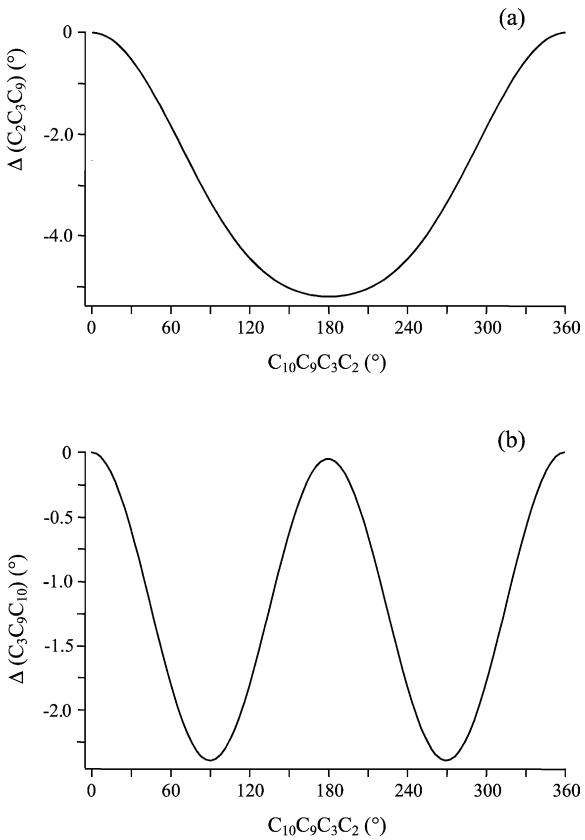

Fig. 7. Dependence of the $(C_2C_3C_9)$ (a) and $(C_3C_9C_{10})$ (b) bond-angles on the $(C_{10}C_9C_3C_2)$ dihedral, within the caffeic acid molecule. (B3LYP/6-31G** level of calculation).

Table 2
Calculated vibrational wavenumbers (cm^{-1}) for the most stable conformers of caffeic acid (at the B3LYP/6-31G** level)

CA 1	CA 2	CA 3	Approximate description[a]
3693(61; 98)[b]	3695(68;117)	3691(107;245)	OH stretching (ring)
3627(123;177)	3629(130;196)	3640(95;88)	OH stretching (ring)
3619(89;193)	3620(88;192)	3619(85;200)	OH stretching
3095(6;169)	3096(9;151)	3097(4;60)	CH sym. stretching (ring)
3084(11;36)	3090(2;17)	3087(4;8)	CH antisym. stretching (ring)
3073(5;62)	3080(6;36)	3079(7;103)	CH_2 stretching
3058(8;25)	3047(12;88)	3051(18;107)	CH stretching (ring)
3049(1;31)	3041(0;5)	3047(1;37)	CH stretching
1741(270;87)	1739(262;88)	1740(262;73)	C=O stretching
1630(208;699)	1632(181;681)	1631(226;801)	C=C stretching
1599(271;1481)	1599(141;993)	1605(162;1261)	CC stretching (ring)
1584(29;22)	1582(253;592)	1582(4;2)	CC stretching (ring)
1512(178;2)	1514(176;10)	1500(249;4)	CC stretching (ring)
1436(177;144)	1431(16;3)	1457(7;136)	CC stretching (ring)
1379(128;35)	1371(16;88)	1364(48;26)	OH (ring/carbox.) ip bending + CC stretching (ring).
1344(31;2)	1353(127;8)	1337(80;7)	OH (ring/carbox.) ip bending
1314(0;43)	1313(22;35)	1310(153;50)	CC stretching (ring) + CH ip bending + OH ip bending
1295(18;6)	1288(306;95)	1295(102;14)	CH ip bending + CC stretching (ring)
1277(379;32)	1278(103;18)	1279(292;114)	CC stretch (ring) + C–O stretch (ring) + CH ip bending
1250(10;94)	1262(57;65)	1248(18;75)	CH ip bending + OH ip bending (carbox.)
1223(4;7)	1220(37;22)	1215(54;6)	CH ip bending + OH ip bending (carbox./ring)
1173(145;118)	1178(133;124)	1182(47;4)	CH ip bending + OH ip bending (ring)
1147(5;47)	1154(21;2)	1151(21;86)	CH ip bending + OH ip bending (ring)
1129(129;7)	1133(162;38)	1133(35;3)	CH ip bending + OH ip bending (ring)
1108(625;201)	1107(613;238)	1112(300;115)	C–O stretching (carbox.) + CH ip bending
1091(128;30)	1087(95;2)	1088(443;113)	CH ip deformation + OH ip deformation
992(21;3)	992(21;3)	992(22;3)	CH op bending
957(15;8)	938(26;9)	958(31;7)	CC stretching + CH ip bending + OH ip bending
930(15;6)	934(5;6)	930(12;5)	CC stretching (ring)
907(1;3)	908(1;2)	880(2;5)	CH op bending (ring/linear chain)
843(5;10)	848(4;13)	851(0;7)	CH op bending (ring/linear chain)
811(48;1)	814(49;1)	842(25;5)	CH op bending (ring)
796(14;6)	797(12;5)	781(20;22)	CH op bending (ring)
785(5;29)	781(9;28)	772(48;4)	CC stretching (ring)
747(9;8)	757(13;9)	747(3;9)	CC stretching (ring)
721(24;3)	722(25;3)	721(19;4)	CCC op deformation (linear chain)
666(6;0)	668(6;0)	665(5;0)	op bending (ring) + OH op bending (carbox.)
625(22;13)	631(27;6)	625(20;13)	CC stretching (ring) + OH ip bending (carbox.)
603(69;4)	601(78;5)	607(57;4)	CH op bending (ring) + OH op bending (carbox.)
579(28;5)	577(16;4)	579(1;7)	OH ip bending (ring)
560(26;4)	556(17;2)	562(38;4)	OH ip bending (carbox.)
528(46;1)	549(40;4)	528(68;1)	CC stretching (ring) + OH ip bending (carbox.)
498(12;1)	495(24;0)	498(15;1)	CCC ip deformation + OH ip bending (carbox.)
454(76;3)	452(52;3)	440(10;0)	OH op bending (ring)
439(13;3)	434(29;0)	436(17;1)	OH op bending (ring) + CH op bending (ring)
427(6;0)	422(21;3)	416(53;1)	op def. (ring)/O_7H_{18} op def.
381(1;2)	380(1;3)	396(1;3)	CCC op deformation (ring + linear chain)
303(4;0)	315(3;0)	351(5;0)	COH ip deformation (ring)
290(4;2)	279(4;5)	301(0;2)	Ip deformation (ring + linear chain)
247(10;4)	273(4;0)	267(94;2)	Op deformation (ring + linear chain)
216(139;1)	226(0;3)	243(78;5)	OH op deformation (ring)

(*continued on next page*)

Table 2 (*continued*)

CA 1	CA 2	CA 3	Approximate description[a]
205(2;5)	221(153;2)	213(0;4)	Op deformation (ring + linear chain)
187(15;0)	183(9;5)	196(0;0)	Chain torsions
134(0;2)	140(0;1)	139(1;2)	Chain torsions
84(0;0)	88(1;0)	87(1;0)	Chain torsions
65(0;0)	69(0;1)	68(0;1)	Chain torsions
37(0;0)	37(2;0)	38(3;0)	Chain torsions

[a] ip and op stand for in-plane and out-of-plane, respectively.
[b] Wavenumbers above 400 cm^{-1} are scaled by a factor of 0.9614 [33]. (IR intensities in km mol^{-1}; Raman scattering activities in Å amu^{-1}).

($C_2C_3C_9$) displays a minimum (118.5°) for ($C_{10}C_9C_3C_2$) equal to 180° (Fig. 7(a)), in order to reduce the steric repulsion between hydrogens $H_{16}\cdots H_{20}$. In turn, for ($C_{10}C_9C_3C_2$) = 0° the ($C_2C_3C_9$) angle has a larger value (123.5°), in order to increase the $H_{15}\cdots H_{20}$ distance. As for the variation of the ($C_3C_9C_{10}$) bond-angle, the highest values are found for ($C_{10}C_9C_3C_2$) = 0° (124.5°) and 180° (128.0°) (Fig. 7(b)), due to the steric hindrance between atoms $H_{15}\cdots H_{20}$ and $H_{16}\cdots H_{20}$, respectively. These repulsive interactions are reduced to a minimum for ($C_{10}C_9C_3C_2$) = 90° and 270°, thus yielding the smallest ($C_3C_9C_{10}$) angle (122.4°).

The vibrational spectrum was calculated for all conformers found for caffeic acid (data available from the authors upon request). The calculated wavenumbers for the most stable geometries —CA 1, CA 2 and CA 3 —are comprised in Table 2, along with the corresponding assignment, and show a good overall accordance with the theoretical values reported by Bakalbassis et al., for CA 1 [18]. Also, the agreement between the presently calculated frequencies, using the scaling factors proposed by Scott and Radom [33], and the Raman experimental data found in the literature for this molecule [37–39] was found to be quite good.

4. Conclusions

The conformational analysis carried out for caffeic acid in the present work, by ab initio methods, yielded fourteen distinct conformers, varying in the orientation of both the pendant arm ring substituent and the phenolic hydroxyl groups, as well as in the geometry of the terminal carboxylate. The corresponding calculated relative energies indicate a clear preference for a planar geometry of the molecule, i.e. for a completely conjugated system, strongly stabilised through π-electron delocalisation. The few deviations found from the planar structure are explained by the occurrence of strong steric hindrance in the planar conformations. Potential-energy profiles for internal rotation around different bonds within the molecule also support the energetically favoured planar arrangement. Three of the calculated conformers for caffeic acid were found to be significantly more stabe then the rest CA 1 (ΔE = 0 kJ mol^{-1}), CA 2 (ΔE = 0.9 kJ mol^{-1}) and CA 3 (ΔE = 1.7 kJ mol^{-1}) with relative populations of 33, 24 and 16%, respectively.

This kind of conformational analysis, based on theoretical methods, may be of significance in future studies aiming at the elucidation of the structure-activity relationships associated with the biological role of certain types of compounds displaying potential therapeutic activity (namely anticancer properties). In fact, they may yield relevant information, at the molecular level, which will allow a complete assignment of the corresponding experimental vibrational data, and hopefully a better understanding of the mechanisms underlying the antiproliferative and cytotoxic activity displayed by several of these phenolic acids. In fact, cytotoxicity evaluation of several such compounds, in different human cancer cells, are already in course in our laboratory (in a parallel study).

Acknowledgements

EVB acknowledges the Erasmus/Socrates student exchange program which allowed her to develop research work at the Molecular Physical-Chemistry Group of the Faculty of Science and Technology of the University of Coimbra (Portugal).

References

[1] V.L. Singleton, Am. J. Enol. Vitic. 38 (1987) 69.
[2] P. Groupy, A. Fleuriet, M.J. Amiot, J.J. Macheix, J. Agric. Food Chem. 39 (1991) 92.
[3] M. Brenes-Balbuena, P. García-García, A. Garrido-Fernandez, J. Agric. Food. Chem. 40 (1992) 1192.
[4] A. Serrano, C. Palacios, G. Roy, C. Cespón, M.L. Villar, M. Nocito, P. González-Porqué, Arch. Biochem. Biophys. 350 (1) (1998) 49.
[5] F.A.M. Silva, F. Borges, M.A. Ferreira, J. Agric. Food Chem. 49 (2001) 3936.
[6] S. Passi, M. Picardo, M. Nazzaro-Porro, Biochem. J. 245 (1987) 537.
[7] T. Nakayama, Cancer Res. (Suppl.) 54 (1994) 1991.
[8] E. Sergediene, K. Jonsson, H. Szymusiak, B. Tyrakowska, I.M.C.M. Rietjens, N. Cenas, FEBS Lett. 462 (1999) 392.
[9] M. Inoue, N. Sakaguchi, K. Isuzugawa, H. Tani, Y. Ogihara, Biol. Pharm. Bull. 23 (10) (2000) 1153 and refs. therein.
[10] G. Roy, M. Lombardía, C. Palacios, A. Serrano, C. Cespón, E. Ortega, P. Eiras, S. Lujan, Y. Revilla, P. González-Porqué, Arch. Biochem. Biophys. 383 (2) (2000) 206 and refs. therein.
[11] T. Gao, Y. Ci, H. Jian, C. An, Vib. Spec. 24 (2000) 225.
[12] H. Esterbauer, J. Gebicki, H. Puhl, G. Jurgens, Free Rad. Biol. Med. 13 (1992) 341.
[13] B. Halliwell, J.C. Gutteridge, Free Radicals in Biology and Medicine, Oxford Science Publications, 1999.
[14] K. Tanaka, S. Sakai, S. Tomiyama, T. Nishiyama, F. Yamada, Bull. Chem. Soc. Jpn 64 (9) (1991) 2677.
[15] S. Tomiyama, S. Sakai, T. Nishiyama, F. Yamada, Bull. Chem. Soc. Jpn 66 (1) (1993) 299.
[16] I. Vedernikova, E. Proinov, D.R. Salahub, A. Haemers, Int. J. Quant. Chem. 77 (1999) 161.
[17] P. Rajan, I. Vedernikova, P. Cos, D. Vanden Berghe, K. Augustyns, A. Haemers, Bioorg. Med. Chem. Lett. 11 (2001) 215.
[18] E. Bakalbassis, A. Chatzopoulou, V.S. Melissas, M. Tsimidou, M. Tsolaki, A. Vafiadis, Lipids 36 (2) (2001) 181.
[19] M. J. Frisch, G. W. Trucks, H. B. Schlegel, G. E. Scuseria, M. A. Robb, J. R. Cheeseman, V. G. Zakrzewski, J. A. Montgomery, Jr., R. E. Stratmann, J. C. Burant, S. Dapprich, J. M. Millam, A. D. Daniels, K. N. Kudin, M. C. Strain, O. Farkas, J. Tomasi, V. Barone, M. Cossi, R. Cammi, B. Mennucci, C. Pomelli, C. Adamo, S. Clifford, J. Ochterski, G. A. Petersson, P. Y. Ayala, Q. Cui, K. Morokuma, D. K. Malick, A. D. Rabuck, K. Raghavachari, J. B. Foresman, J. Cioslowski, J. V. Ortiz, A.G. Baboul, B. B. Stefanov, G. Liu, A. Liashenko, P. Piskorz, I. Komaromi, R. Gomperts, R. L. Martin, D. J. Fox, T. Keith, M. A. Al-Laham, C. Y. Peng, A. Nanayakkara, C. Gonzalez, M. Challacombe, P. M. W. Gill, B. Johnson, W. Chen, M.W. Wong, J. L. Andres, C. Gonzalez, M. Head-Gordon, E. S. Replogle, and J. A. Pople, Gaussian 98 - Revision A. 7, Gaussian Inc., Pittsburgh PA, 1998.
[20] T.V. Russo, R.L. Martin, P.J. Hay, J. Phys. Chem. 99 (1995) 17085.
[21] A. Ignaczak, J.A.N.F. Gomes, Chem. Phys. Lett. 257 (1996) 609.
[22] F.A. Cotton, X. Feng, J. Am. Chem. Soc. 119 (1997) 7514.
[23] A. Ignaczak, J.A.N.F. Gomes, J. Electroanal. Chem. 420 (1997) 209.
[24] T. Wagener, G. Frenking, Inorg. Chem. 37 (1998) 1805.
[25] F.A. Cotton, X. Feng, J. Am. Chem. Soc. 120 (1998) 3387.
[26] C. Lee, W. Yang, R.G. Parr, Phys. Rev. B37 (1988) 785.
[27] B. Miehlich, A. Savin, H. Stoll, H. Preuss, Chem. Phys. Lett. 157 (1989) 200.
[28] A. Becke, Phys. Rev. A38 (1988) 3098.
[29] A. Becke, J. Chem. Phys. 98 (1993) 5648.
[30] P.C. Hariharan, J.A. Pople, Theor. Chim. Acta 28 (1973) 213.
[31] M.M. Francl, W.J. Pietro, W.J. Hehre, J.S. Binkley, M.S. Gordon, D.J. DeFrees, J.A. Pople, J. Chem. Phys. 77 (1982) 3654.
[32] C. Peng, P.Y. Ayala, H.B. Schlegel, M.J. Frisch, Comp. Chem. 17 (1996) 49.
[33] A.P. Scott, L. Radom, J. Phys. Chem. 100 (1996) 16502.
[34] L. Radom, W.J. Hehre, J.A. Pople, J. Am. Chem. Soc. 94 (1972) 2371.
[35] L.A.E. Batista de Carvalho, A.M. Amorim da Costa, J.J.C. Teixeira-Dias, J. Mol. Struct. (Theochem) 205 (1990) 327.
[36] S. García-Granda, G. Beurskens, P.T. Beurskens, T.S.R. Krishna, G.R. Desiraju, Acta Cryst. C43 (1987) 683.
[37] S. Sánchez-Cortés, J.V. García-Ramos, Spectrochim. Acta A55 (1999) 2935.
[38] S. Sánchez-Cortés, J.V. García-Ramos, Appl. Spec. 54 (2) (2000) 230.
[39] S. Sánchez-Cortés, J.V. García-Ramos, J. Colloid Interface Sci. 231 (2000) 98.